THE JOURNAL OF PHYSICAL CHEMISTRY B

Article

pubs.acs.org/JPCB

# Effects of Solvent Properties on the Spectroscopy and Dynamics of Alkoxy-Substituted PPV Oligomer Aggregates

Woong Young So,[†] Jiyun Hong,[†] Janice J. Kim,[†] Gizelle A. Sherwood,[†] Kelly Chacon-Madrid,[†,§] James H. Werner,[‡] Andrew P. Shreve,[‡,∥] and Linda A. Peteanu*[,†]

[†]Department of Chemistry, Carnegie Mellon University, 4400 Fifth Avenue, Pittsburgh, Pennsylvania 15213, United States

[‡]Materials Physics and Applications Division, Center for Integrated Nanotechnologies, Los Alamos National Laboratory, Los Alamos, New Mexico 87545, United States

Jurjen Wildeman

Zernike Institute for Advanced Materials, University of Groningen, Nijenborgh 4, 9747 AG Groningen, The Netherlands

Supporting Information

**ABSTRACT:** Conjugated systems are frequently studied in their nanoaggregate form to probe the effects of solvent and of film formation on their spectral and dynamical properties. This article focuses on the emission spectra and dynamics of nanoaggregates of alkoxy-substituted PPV oligomers with the goal of interpreting the vibronic emission envelopes observed in these systems (*J. Phys. Chem. C* **2009**, *113*, 18851−18862). The aggregates are formed by adding a nonsolvent such as methanol (MeOH) or water to a solution of the oligomers in a good solvent such as methyl tetrahydrofuran (MeTHF) or tetrahydrofuran (THF). The emission spectra of aggregates formed using either of these combinations exhibit a vibronic pattern in which the ratio of the intensity of highest-energy band to that of the lower energy peaks depends strongly on the ratio of good to poor solvent. In aggregates formed from MeTHF:MeOH, this was shown to be due to the presence of both aggregate-like and monomer-like emitters forming a "core" and surrounding "shell"-like structure, respectively, within a single aggregate (*J. Phys. Chem. C* **2011**, *115*, 15607−15616). In support of this model, the monomer-like emission is shown here to be significantly decreased by changing the solvent pair to the more polar THF:water. This suggests that nanoaggregates formed in THF:water contain a much smaller proportion of monomer-like chains than those formed in MeTHF/MeOH, as would be expected from using a more highly polar nonsolvent. Results from bulk steady-state and time-resolved emission measurements as well as fluorescence lifetime imaging microscopy (FLIM) of the aggregates are shown to be consistent with this interpretation.

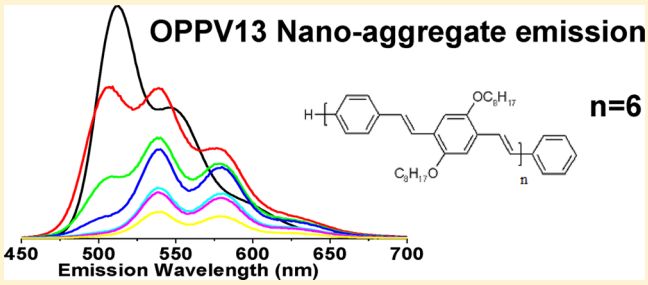


## INTRODUCTION

Recent years have seen an upsurge in applications using fluorescent conjugated polymers such as MEH-PPV in diverse areas from display technologies and solar cells to schemes for highly sensitive analyte detection.[1,2] Optimization for these and future uses requires an understanding of how morphological effects, such as aggregation, impact important functional features including emission wavelength and intensity and charge migration. In fact, studies have implicated aggregates in polymer films as key players in both unfavorable properties, such as emission quenching, and in desirable properties, such as enhanced charge transport.[3] Because even a small number of aggregated chains can adversely affect the overall operation of a device, tools to detect the presence of aggregated chromophores in complex mixtures and in relatively large-area solid films have become increasingly important. Optical-based imaging methods such as Raman, near- and far-field fluorescence, and fluorescence lifetime imaging microscopy (FLIM) are particularly well-suited to this purpose.[4−11] However, these strategies rely on a detailed knowledge of how the optical signatures of the aggregated and isolated chains differ.

One approach to identify the spectral signatures of aggregation is through the use of "solvent poisoning" or creating aggregated chains in solution suspension by adding a poor solvent to a solution of the molecule of interest dissolved in a good solvent.[12−17] This allows the properties of isolated and aggregated chains to be compared using the same spectroscopic techniques and under similar conditions. Also

**Special Issue:** Richard A. Mathies Festschrift

**Received:** February 28, 2012
**Revised:** June 5, 2012
**Published:** June 21, 2012

important to this effort are the various theoretical models that have been developed for understanding the effects of aggregation on spectral line shape.[18−21]

The focus of this contribution is on the spectroscopy, morphology, and dynamics of aggregates composed of model oligomers related to the electroluminescent polymer MEH-PPV (Chart 1) that are formed by a solvent reprecipitation method. An important rationale for studying aggregates of oligomers (7−13 rings) is that the spectral and dynamical effects due to aggregation can be better separated from those due to structural defects or multiple conjugation lengths such as are typically found in the polymer.[22−24] We have previously reported on the properties of aggregates formed from these oligomeric model compounds using methyl tetrahydrofuran (MeTHF) and methanol (MeOH) as the good and poor solvents, respectively.[8,25] In this work, we showed that the changes in emission spectrum and lifetime that had been reported for MEH-PPV upon aggregation are effectively mimicked by aggregates made from the longer-chain oligomers (OPPV13). The bulk emission spectra and fluorescence dynamics of these oligomer aggregates showed evidence of both monomer-like (noninteracting) and aggregate-like chains.[25] Follow-up morphological studies of individual aggregates using FLIM confirmed that each aggregate contains both types of chains assembled in a "core−shell" structure in which the aggregate chains lie at the center and the monomer-like chains lie at the periphery.[8] Here we use the term monomer-like to indicate that these chains are associated with the aggregate surface (as shown by imaging results below and in ref 8) and to distinguish these emitters from chains that are free in solution or surrounded by good solvent. As would be expected, the ratio of monomer-like to aggregate-like chains is tunable by changing the relative percentages of good and poor solvent in the mixture.

**Chart 1. OPPV Oligomer Structures Used in This Work**[a]

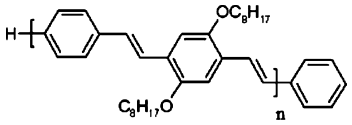


[a] $n$ = 3 for OPPV7 and $n$ = 6 for OPPV13.

Here we explore the effects of inducing aggregation of OPPVs using a solvent pair with a greater polarity difference, namely, tetrahydrofuran (THF) and water. The fluorescence spectra, morphologies, and emission dynamics of the aggregates formed in THF:water are consistent with their having stronger chain−chain interactions than those formed from MeTHF:-MeOH. In particular, isolated monomer-like chains are strongly disfavored in the more polar THF:water environment, and this has observable consequences on the emission properties and morphology of the aggregates formed.

## EXPERIMENTAL SECTION

The methods used here are those detailed in refs 8 and 25, with the exception that the solvent pair used here is THF:water. In brief, aggregates were prepared via a reprecipitation method in which various volumes of a $\mu$M stock solution in THF were added to water such that the final volume was 1 mL. The size distributions of the resulting aggregates were determined by dynamic light scattering (DLS) using a Malvern Zetasizer Nanoseries ZS instrument. Prior to and following the addition of water, the absorption and emission spectra of the samples were obtained using a Cary 50 UV−visible spectrophotometer and a FluoroMax-2 Jobin Yvon SPEX spectrofluorimeter, respectively. Both the monomer and aggregate emission spectra were obtained at the absorption maximum of the monomer (450 nm). When indicated, the emission intensity of the aggregate suspension was scaled to account for any differences in the extinction of the aggregate versus the monomer at this wavelength. Bulk emission lifetimes were obtained by excitation with a 437 nm pulsed diode laser (LDH-PC-440, PicoQuant), and the decays were recorded using time-correlated single-photon counting electronics (PicoHarp300, Picoquant). The emission was detected using a single photon avalanche photodiode (MPD) with filters used for wavelength selection (Thorlabs).

The FLIM system used at the Center for Integrated Nanotechnologies (CINT) consists of a pulsed diode laser operating at 440 nm (LDH-PC-440, Picoquant), time-correlated single-photon counting electronics (Picoharp 300, Picoquant), a scanning sample stage (PI, model P-733.3CD), an inverted microscope (Olympus, IX71), and a single-photon counting avalanche photodiode detector (Perkin-Elmer). A commercial software package (SymPhoTime, Picoquant) was used for data acquisition and analysis. The laser power on the

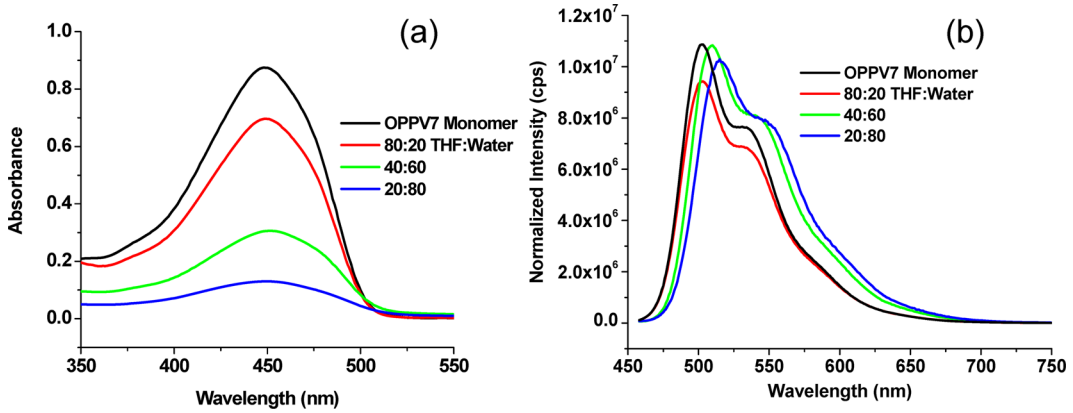


**Figure 1.** Absorbance (a) and emission (b) of OPPV7 monomer and aggregates formed in solutions containing various ratios of THF:water (v:v). The emission spectra are normalized to the absorption at the excitation wavelength (450 nm). Error in the relative intensities is ∼15%.


dx.doi.org/10.1021/jp301971p | J. Phys. Chem. B 2012, 116, 10504−10513

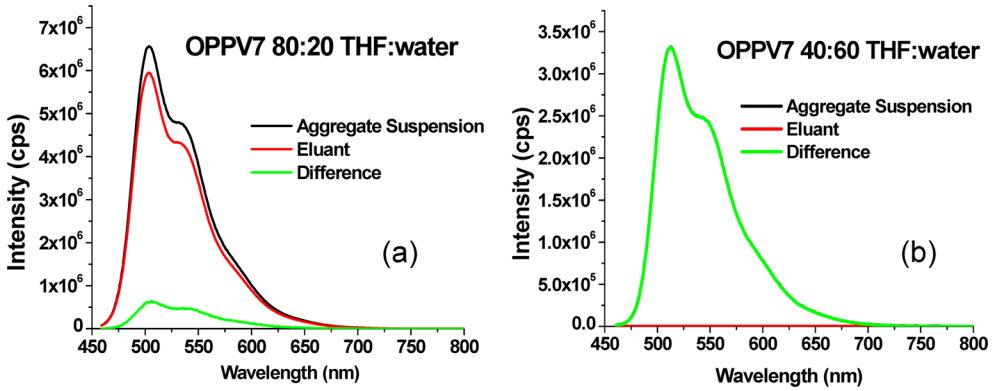


**Figure 2.** Filtration experiments on OPPV7 aggregates formed in solutions formed with (a) 20% water and (b) 60% water in THF. The initially formed aggregate suspension (black line) and the eluant collected following filtration of this suspension through a 200 nm pore syringe filter (red) are shown. The difference of these two spectra (green) represents the emission lost in the eluant due to trapping of aggregates in the filter. In panel b, the green and black spectra overlay exactly because the eluant is completely nonemissive.

sample was <1 $\mu$W, and the sample was held under nitrogen purge during imaging. The emission was wavelength-selected using 10 nm bandpass filters (Thorlabs) centered at the various vibronic peaks of the aggregate emission spectra. An instrument response function (IRF) of 240 ps was measured using the laser light scattered when focusing on a clear region of the microscope slide and collected through a 460 nm short pass filter. All FLIM images shown here are color-coded to reflect the intensity weighted average lifetime.

## RESULTS AND DISCUSSION

The organization of this section is as follows. Three types of data on the aggregates are presented: steady-state absorption and emission spectra, wavelength-resolved fluorescence lifetime measurements, and FLIM images on the picosecond time scale. Comparisons between the data obtained for aggregates formed in THF:water and those from MeTHF:MeOH reveal changes in the morphologies and excited-state dynamics of the aggregates that are induced by increasing the polarity difference between the solvents used to form them. The focus is on aggregates formed from two oligomers, relatively short-chain (7 rings, OPPV7) and long-chain (13 rings, OPPV13) species. Previous studies by our group have shown significant differences in the behavior of shorter (3−7 ring) versus longer (9−13 ring) oligomers upon aggregation in MeTHF:MeOH.[8,25] This study considers the effect of increasing aggregation (increasing poor solvent) on the emission spectra, lifetimes, and morphology, as revealed by FLIM. A more detailed treatment of the vibronic spectra of the aggregates is deferred to a forthcoming contribution.

Here we first discuss aggregates formed from the shorter-chain oligomer OPPV7. Although the absorption spectrum of the monomer is relatively unstructured, the emission spectrum shows a short progression in the C═C stretching mode (Figure 1). Adding small amounts of water (20% by volume or less) does not alter the band shape of either spectrum or significantly change the emission intensity. At this THF:water ratio, the DLS spectrum shows two peaks, one centered at ∼250 nm and one between 1 and 10 nm (Figure S1a of the Supporting Information). Increasing the percentage of water induces a small red shift (620 $cm^{-1}$) in the OPPV7 emission spectrum, although the shape of the absorption spectrum is nearly unchanged (Figure 1). When this occurs, the DLS shows a single peak at ∼250 nm (Figure S1c of the Supporting Information). The effects of aggregation on the emission spectrum of OPPV7 in THF:water, although small, are more noticeable than those previously obtained when using the MeTHF:MeOH solvent pair.[25] In the latter case, the absorption and emission spectra of the mixed solvent suspensions are identical to those of the monomer even at the highest percentages of MeOH used (80−90%).

One indication of the interchain interaction strength in these aggregates is the ease with which they can be dissociated by passing the mixed solvent suspension through a 200 nm pore syringe filter (see refs 25 and 26). This is measured by comparing the emission spectrum and intensity of the eluant (the solution that passes through the filter) to that of the original suspension prior to filtering.[25,26] If the original suspension contains a large fraction of unaggregated chains, then the eluant emission spectrum will be essentially identical to that of the monomer itself. This is also the case if the suspension contains weakly bound aggregates that are dissociated by the filtration process. Clearly, aggregates smaller than the filter pore size should also pass through unobstructed. Larger or more strongly bound aggregates are trapped in the filter, generally resulting in a less emissive eluant. Between these extremes, various proportions of trapped and dissociated aggregates can be identified by comparing the emission spectra of the eluant to that of original suspension. In all cases, the same general trends are observed if the *absorption* of the eluant is monitored rather than its *emission*. This means that the loss of emission upon filtration is not solely due to a difference in the quantum yields between the species in the original suspension and those that pass through the filter (data not shown). Filtering solutions of oligomers in a good solvent gives rise to an eluant with an emission spectrum identical in shape and intensity to that of the unfiltered solution. This indicates that the interactions between the monomeric form and the filter are minimal.

When suspensions of OPPV7 containing the smallest proportion of water in THF (20−40%, Figure 1b) are filtered, the emission spectrum of the resulting eluant is identical in shape and similar in intensity to that of the solution prior to filtering (Figure 2a). The DLS of the eluant shows that the peak previously observed at ∼250 nm has vanished, leaving only a peak at ∼2 nm (Figure S1b of the Supporting Information). Increasing the proportion of water in the solution decreases the amount of eluant fluorescence observed until, at 40% water or


dx.doi.org/10.1021/jp301971p | J. Phys. Chem. B 2012, 116, 10504−10513

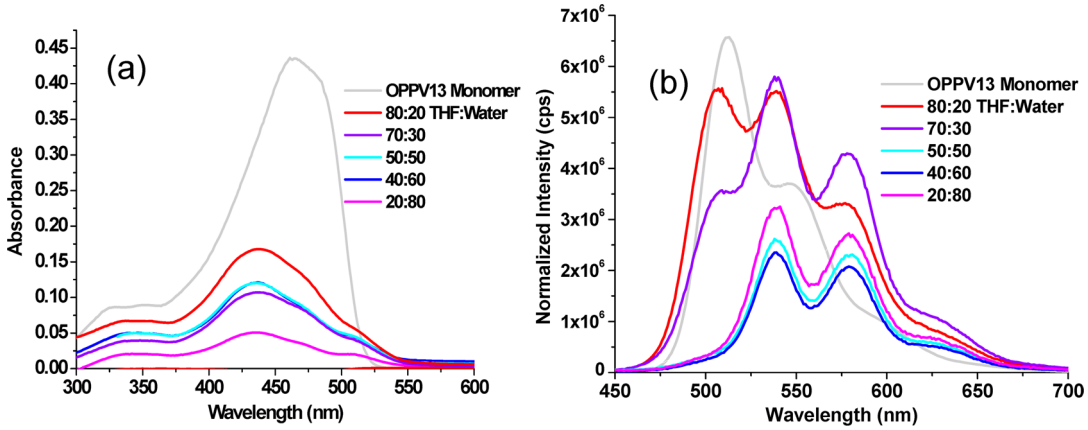


**Figure 3.** (a) Absorbance and (b) emission of OPPV13 monomer and aggregates formed in solutions containing various ratios of THF:water (v:v). The emission spectra are normalized to the absorption at the excitation wavelength (450 nm), and the emission of the monomer is divided by 3.

higher, the eluant is completely nonemissive (Figure 2b). This shows that the degree of aggregation increases with increasing proportion of poor solvent, as was inferred from the spectral changes described above. In contrast, when OPPV7 aggregates formed in MeTHF:MeOH (mean size ~200 nm) are filtered, the emission spectra and intensities of the resulting eluants are nearly identical to that of the original suspension, even at over 80% MeOH.[25] This implies that the MeTHF:MeOH aggregates are weakly bound and therefore easily broken apart by the filtration process.

Unlike what is seen for OPPV7, aggregation strongly perturbs the emission properties of the longer-chain oligomer OPPV13. Following the addition of only 20% water to the monomer in THF, the absorption spectrum develops a shoulder at lower energy indicative of aggregation (Figure 3a). At the same time, the emission intensity decreases significantly, and relative intensities of the vibronic bands arising from the C═C stretch are noticeably altered (Figure 3b and Table 1). In particular, there is an apparent shift in intensity from the monomer electronic origin (513 nm) to higher vibronic bands until, at 40% water, the 513 nm band is no longer observed. Increasing the proportion of water beyond this point does not further change either the absorption or emission spectra of the aggregates. By comparison, although the intensity at the monomer origin also diminishes with increasing MeOH concentration in aggregates formed from MeTHF, the proportion of MeOH must be over 80% before this band is no longer observed (Figure 4). At lower MeOH:MeTHF ratios, the emission spectra exhibit complex vibronic envelopes[8,25] similar to those seen in THF:water aggregates when the percentage of water is only 20−30% (compare Figures 3b and 4).

**Table 1. Emission Peak Positions and Relative Intensities for OPPV13 Monomer and THF:Water Aggregates**

| sample | band 1[a] | band 2 | band 3 | band 4 |
|---|---|---|---|---|
| monomer | 513[b] (1.8)[c] | 545 | | |
| 80:20[d] | 508 (1.0) | 538 | 577 (0.60) | 630 (0.14) |
| 70:30 | 508 (0.62) | 538 | 577 (0.74) | 630 (0.16) |
| 60:40 | 506 (0.25) | 538 | 580 (0.79) | 630 (0.18) |
| 50:50 | | 538 | 580 (0.88) | 630 (0.19) |
| 40:60 | | 538 | 580 (0.88) | 630 (0.22) |
| 20:80 | | 538 | 580 (0.85) | 630 (0.21) |

[a]Highest energy band of the monomer. Bands are grouped by wavelength range [b]In nm (±2 nm). [c]Intensity relative to band 2. [d]THF:water ratio used to form aggregates; see the text.

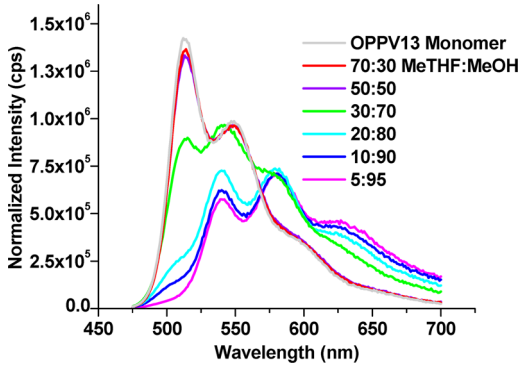


**Figure 4.** Emission of the OPPV13 monomer and aggregates formed in solutions containing various ratios of MeTHF:MeOH (v:v). The emission spectra are normalized to the absorption at the excitation wavelength (450 nm). Excitation wavelength is 450 nm.

Filtration measurements confirm that the vibronic envelopes of the OPPV13 THF:water aggregate emission spectra arise from a mixture of two types of emitters. In Figure 5, the fluorescence spectra of three representative THF:water suspensions (black) are compared to those of the corresponding eluants (red). The spectral shape of the eluant emission is essentially identical to that of the monomer, and its intensity decreases as the percentage of water in the sample increases. This is not surprising because fewer unaggregated chains or very small aggregates, which would pass through the filter and into the eluant, are expected at the higher water percentages.

Further evidence of the presence of two emitting populations is obtained using DLS. The DLS spectra of OPPV13 aggregates formed using higher percentages of THF (>50%) exhibit a bimodal size distribution with one population peaked at a diameter ($d$) > 800 nm, whereas another is peaked at $d \approx 3-5$ nm (Figure S2a of the Supporting Information for 70% THF). The DLS data for THF:water ratios larger than 70% (not shown) indicate that the aggregate size distribution is in flux. In other words, the aggregates appear to be forming and redissolving dynamically on the time scale of the measurement. These conditions correlate to the "mixed" emission spectra previously described. However, at higher proportions of added water, the aggregate size distribution becomes stable and can be


dx.doi.org/10.1021/jp301971p | J. Phys. Chem. B 2012, 116, 10504−10513

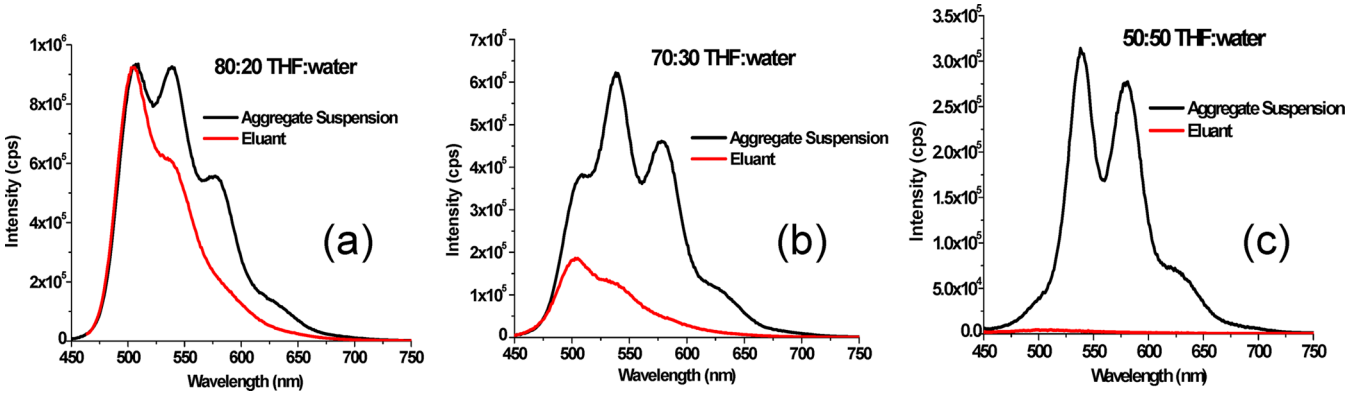


**Figure 5.** Filtration experiments on OPPV13 aggregates formed in solutions formed with (a) 20, (b) 30, and (c) 50% water in THF. The initially formed aggregate suspension (black line) and the eluant collected following filtration of this suspension through a 200 nm pore syringe filter (red) are shown.

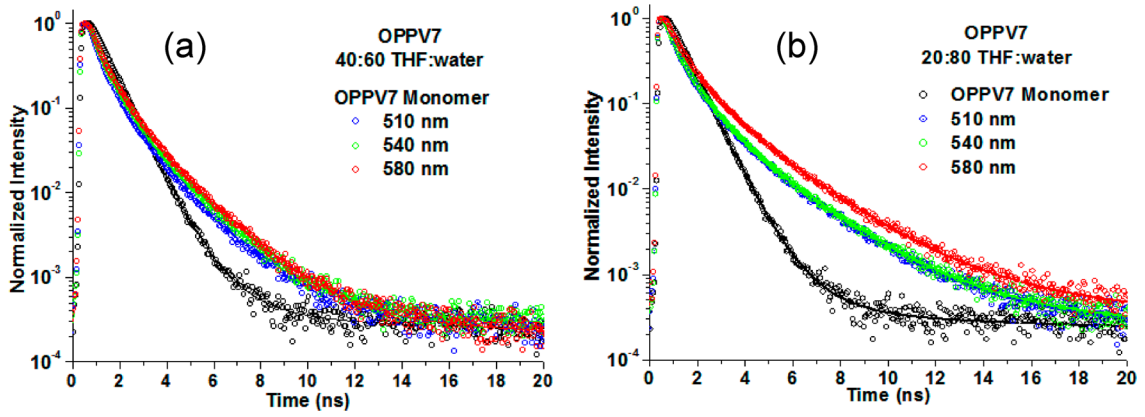


**Figure 6.** Emission decays of OPPV7 in (a) 60 and (b) 80% water in THF. The data are shown in the open circles, and the corresponding fits are shown using solid lines. The wavelengths (10 nm bandpass) correspond to the vibronic peaks of OPPV7. (See Figure 1.)

modeled by a single Gaussian with a mean diameter of ∼150 nm (Figure S2c of the Supporting Information for 40% THF). Under these conditions, the aggregate fluorescence spectra are also consistent with a single type of emitter. In summary, the fact that the complex spectra observed for several THF:water suspensions can be separated into two contributions based on size demonstrates that they are due to a mixture of two distinct species. A similar result was observed in aggregates formed using a MeTHF:MeOH solvent mixture, confirming the universality of this behavior in OPPVs.[25]

Comparing the emission lifetime of the monomer and aggregate species in solution highlights changes in excited-state dynamics due to increased chain−chain interactions. Variations in the lifetime with emission wavelength can be observed in aggregates or other multichromophoric species due to energy transfer between subunits or the presence of multiple subpopulations that differ in their electronic properties. In refs 8 and 25, we showed that the wavelength dependence of the emission lifetime could be used to separate spectral features due to more isolated (monomer-like) chains from those due to aggregated chains. Specifically, for OPPV13 aggregates formed from MeTHF:MeOH, the emission lifetime at the wavelength of the monomer origin (510 nm) is the same as that of the isolated monomer, whereas the longer wavelength emission bands (530−650 nm) have significantly shorter lifetimes characteristic of aggregated chains.

Analogous measurements are reported here for aggregates of OPPV7 and OPPV13 in THF:water. Considering first OPPV7, its measured lifetime is identical to that of the monomer (0.75 ns, 97% of the total amplitude) when the amount of water is 20% or less (data not shown). As the percentage of water increases, the 0.75 ns monomer-like component remains, but a second component (1.5 to 2 ns) grows in until the two are nearly equal in amplitude (Figure 6). Notably, the slower component appears at the same THF:water ratio at which the emission spectrum undergoes a small red shift, suggesting that both phenomena arise from increased chain−chain interactions. As was seen in MeTHF:MeOH, the emission dynamics of OPPV7 in THF:water are essentially the same at all wavelengths probed here. However, one interesting difference between the two systems is that aggregation in OPPV7 leads to an *increase* in the average emission lifetime, whereas the lifetime of the MeTHF:MeOH aggregates is essentially unchanged from that of the monomer. A reason for this increase observed in the solution phase has not yet been determined. However, because it occurs without a loss of vibronic structure in the emission spectrum or significant quenching, classical excimer formation appears to be unlikely.

Turning to OPPV13, the emission lifetimes at low percentages of water (20%) are once again somewhat *longer* than that of the isolated monomer (0.7 ns versus 0.6 ns for the monomer, Figure 7a). Moreover, there is an increase in the contribution of a second component (1 to 1.5 ns) at the redder


dx.doi.org/10.1021/jp301971p | J. Phys. Chem. B 2012, 116, 10504−10513

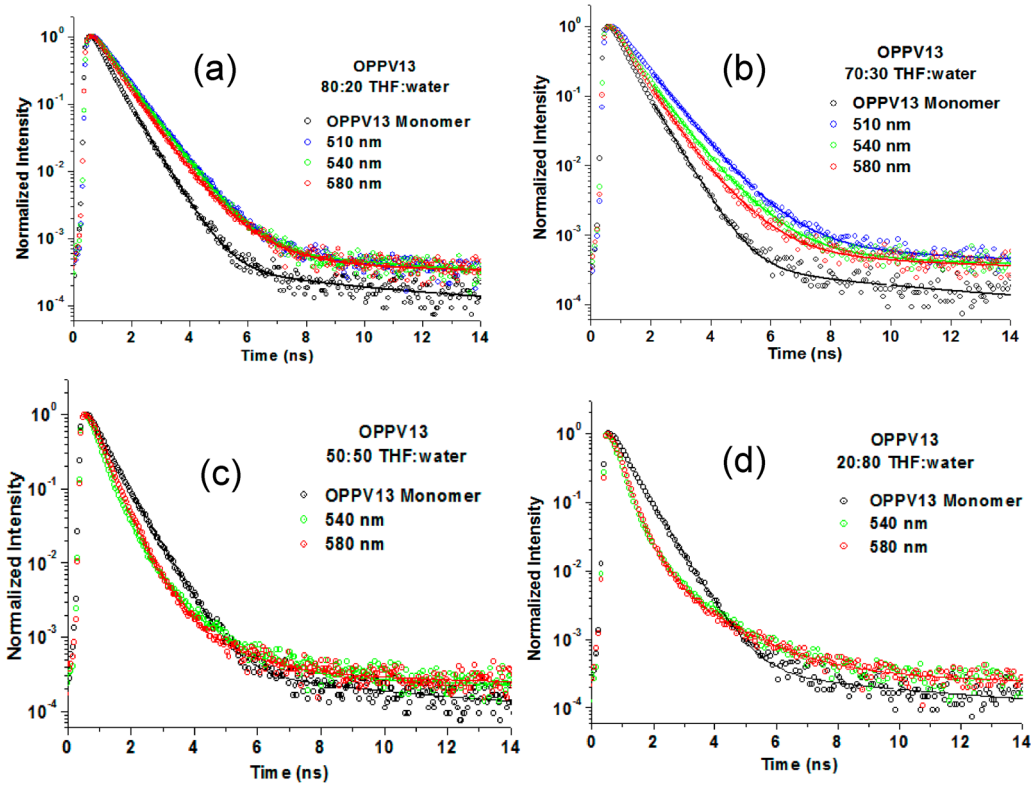


**Figure 7.** Emission decays of OPPV13 in (a) 20, (b) 30, (c) 50, and (d) 80% water in THF. The data are shown in the open circles, and the corresponding fits are shown using solid lines. The wavelengths (10 nm bandpass) correspond to the vibronic peaks of OPPV13. (See Figure 3.)

emission wavelengths. This trend becomes more pronounced when the percentage of water is raised to 30−40%. At 50% THF:water, which is the composition at which the band at 513 nm (Figure 3b) essentially vanishes, there is a sudden *decrease* in the average lifetime such that the dominant component (~60% of the overall amplitude) is now ~0.4 ns. The kinetics are also the same at all emission wavelengths under these conditions. This is consistent with steady-state spectroscopy results that suggest that essentially all of the chains in the sample are now aggregated. Moreover, this shorter lifetime is within the range observed for the aggregated chains using FLIM (see below). We note in passing that the short lifetime observed in the aggregated species does not appear to be due to photodamage because this component is observed under both the weak photoexcitation conditions of bulk solution-phase TCSPC and the higher photon flux conditions of femtosecond upconversion spectroscopy (manuscript in preparation). Moreover, we have not observed an increase in the relative contribution of this fast component at higher powers or when the sample is exposed to air.

Overall, the spectral results for aggregates formed in THF:water support our earlier assertion[8,25] that the vibronic envelopes observed for these aggregates under some conditions reflect a heterogeneous mixture of monomer-like and aggregate-like chains. When the contribution of monomer-like chains is decreased, as in the case in the more polar THF:water mixture, the vibronic spectra of the resulting aggregates are more characteristic of a single type of emitter.

One possible reason that both monomer-like and aggregate-like chains would be observed in an aggregate suspension is that these are two distinct subpopulations within the bulk sample. Another possibility is that each individual aggregate in the suspension contains both types of chains with varying proportions depending on the nature of the solvent environment. We have previously shown that the latter picture is correct for aggregates formed from MeTHF:MeOH using FLIM.[8] Here we extend that work to the THF:water aggregate system and again demonstrate that the images derived from FLIM are consistent with the presence of two types of emitters within the same discrete aggregate structure.

In brief, the FLIM experiment is performed by imaging the fluorescence of a single aggregate through a series of 10 nm bandpass filters coincident with the vibronic peaks in the monomer and aggregate emission spectra (i.e., 510, 540, and 580 nm in OPPV13, see Figures 3 and 4). A spatial variation in the emission lifetime of OPPV13 aggregates formed from MeTHF:MeOH is observed (Figure 8) such that the chains at the periphery have longer emission lifetimes than those at the center of the structure. Moreover, the longer-lived chains are brightest when the emission is collected at 510 nm, whereas the shorter-lived chains predominate for 540 and 580 nm. These images are consistent with a "core−shell" aggregate structure in which the more highly packed chains lie at the center ("core") and the monomer-like chains lie at the periphery ("shell").

In OPPV13 aggregates formed from a solution that is 70% THF and 30% water, a similar "core−shell" structure is evident with a decreased contribution from the longer-lived chains as the wavelength increases from 510 to 580 nm (Figure 9). In these images, the intensity at 510 nm is only a factor of 3 lower than that at 540 nm due to a relatively high population of monomer-like chains. As the proportion of water is increased to 60%, several changes are observed (Figure 10). First, the emission intensity of the aggregate at 510 nm drops to less than 10% of that at 540 nm, consistent with the loss of this band in the bulk emission spectrum. (See Figure 3b.) The overall distribution of the emission lifetimes at each wavelength also


dx.doi.org/10.1021/jp301971p | J. Phys. Chem. B 2012, 116, 10504−10513

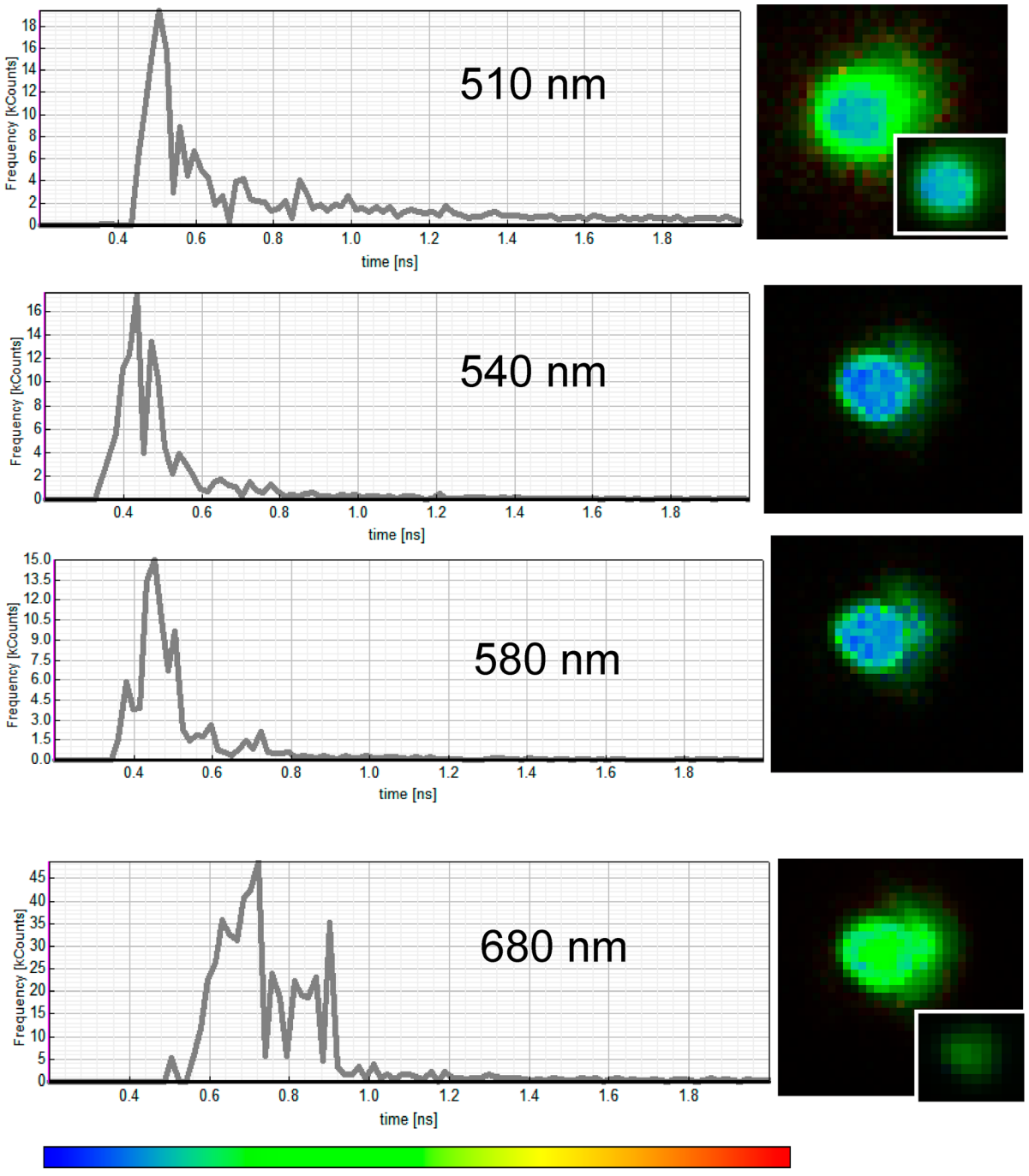


**Figure 8.** FLIM images of a single aggregate formed from 90% MeOH in MeTHF. Images were obtained by collecting emission at each of the vibronic peaks of the emission spectrum (510, 540, 580 nm, see Figure 4) with a 10 nm band-pass filter and at 680 nm using a 30 nm band-pass filter. The insets at 510 and 680 nm display the intensities of the aggregate when the images are scaled identically to those obtained at 540 and 580 nm. The graphs show the distribution of the average lifetime in the image, and the color scale (0.2 to 2 ns) is given. Pixel size is 0.1 $\mu$m.

shifts to shorter values, consistent with what is seen in the bulk emission decays (Figure 7). Similar to the other examples, the longer-lived chains tend to cluster at the periphery. However, the ratio of "shell" to "core" emission in these aggregates is clearly smaller than that in the other examples shown here. This is not surprising given that a higher percentage of water is expected to increase the proportion of oligomers in the aggregated state. Notably, there is also less variation in the lifetime distributions seen in FLIM images obtained at the different vibronic peaks for the 40:60 THF:water aggregates than for those formed in 30:70 THF:water or in MeTHF:-MeOH. For example, comparing the image of the 40:60 THF:water aggregates obtained at 510 nm to that at the longer wavelengths, although the overall *intensity* of the image is much weaker at 510 nm, the distribution of lifetimes is similar to that at the longer wavelengths. In contrast, the images of both the 30:70 THF:water and MeTHF:MeOH aggregates are notably different at 510 nm from those at 580 nm. These results are consistent with the bulk emission lifetime measurements (Figure 7) in which the wavelength dependence of the decays is less evident as the proportion of water increases. It is also consistent with the filtration results (Figure 5), which suggest


dx.doi.org/10.1021/jp301971p | J. Phys. Chem. B 2012, 116, 10504−10513

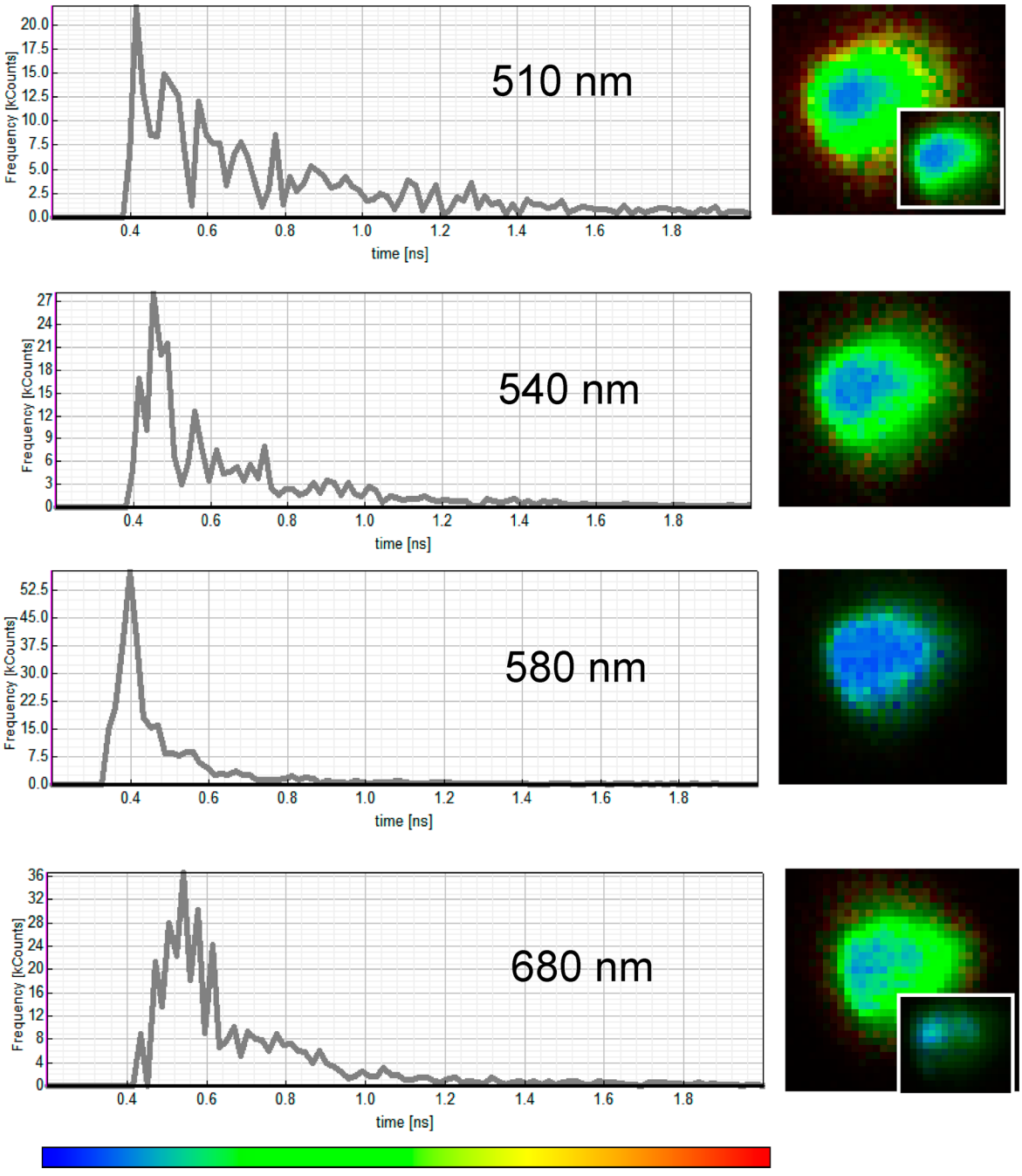


**Figure 9.** FLIM images of a single aggregate formed from 30% water in THF. (See Figure 3.) Refer to caption of Figure 8 for details.

that the sample becomes more uniformly aggregated with increased addition of water.

In conclusion, the spectroscopic properties and the structures of OPPV aggregates formed using the solvent mixtures with a greater polarity difference (THF:water) versus a smaller polarity difference (MeTHF:MeOH) are significantly different. These differences can be rationalized by the fact that water is more destabilizing for isolated oligomer chains than is MeOH due to its higher polarity. Consequently, a greater proportion of the chains in the THF:water mixture will be in the aggregated state. These results support our previous assertion[8,25] that the vibronic structure in the emission spectra of OPPV aggregates reflects the fact that each aggregate contains a mixture of monomer-like and aggregate-like chains in varying proportions depending on the amount of nonsolvent present. The imaging results presented here likewise support our previous hypothesis that these two types of chains form a "core−shell" structure with the aggregated chains at the "core"' and the monomer-like chains at the surface ("shell"). Specifically, the FLIM results show that the contribution of "monomer-like" chains to the aggregate structure is significantly less in aggregates formed in THF:water than in MeOH:MeTHF. Again, this is due to the fact that unaggregated chains are more strongly disfavored in THF:water than in MeTHF:MeOH. This work demonstrates that fluorescence lifetime imaging can be used to disentangle the complex emission spectra that characterize aggregates of PPV-based materials and can therefore be used to understand the variations in emission spectra and lifetimes that are commonly observed in film samples.


dx.doi.org/10.1021/jp301971p | J. Phys. Chem. B 2012, 116, 10504−10513

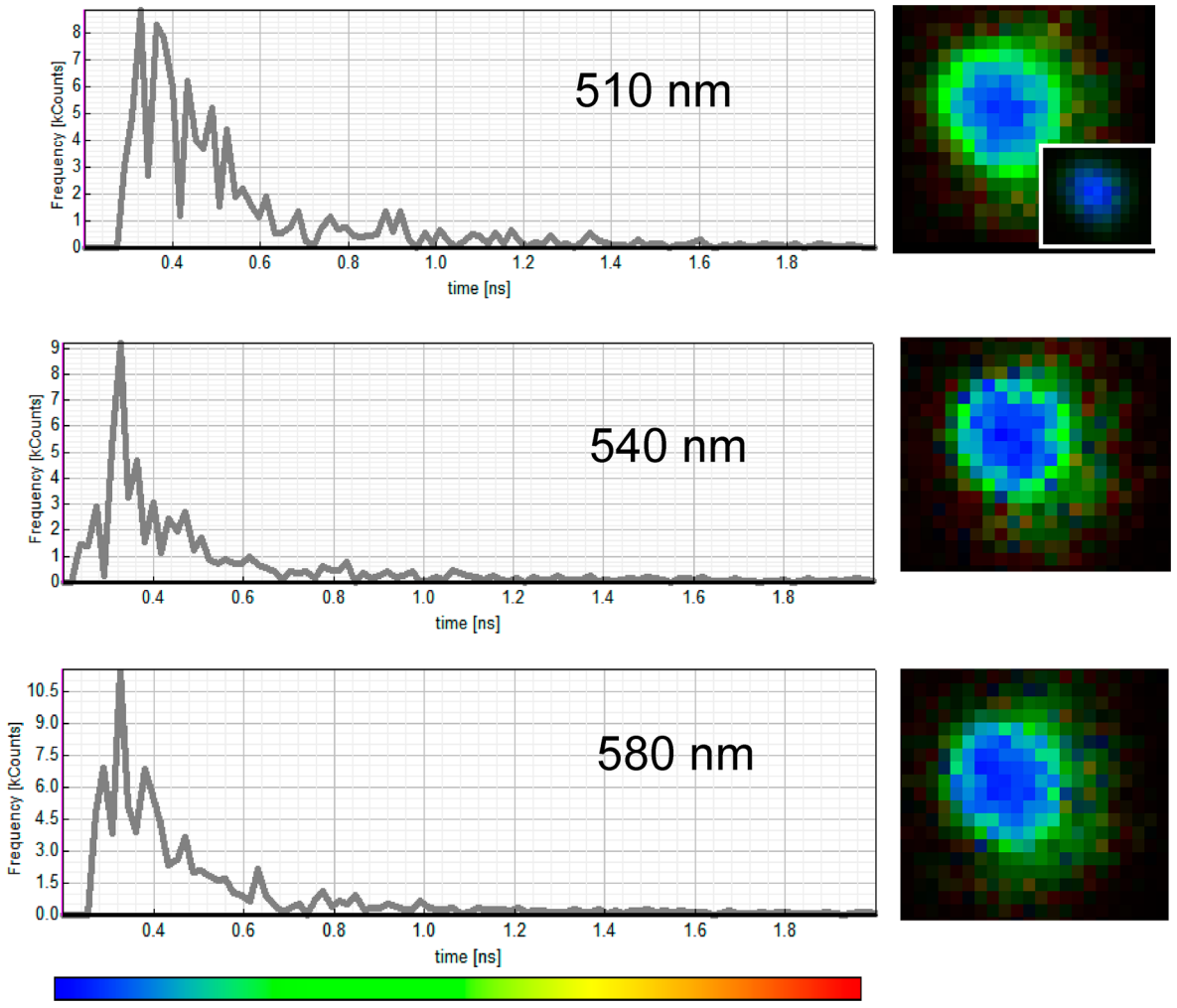


**Figure 10.** FLIM images of a single aggregate formed from 60% water in THF. (See Figure 3.) Refer to caption of Figure 8 for details.

## ■ ASSOCIATED CONTENT

### Supporting Information

DLS spectra for selected OPPV7 and OPPV13 suspensions in THF:water prior to and after filtration are given. This material is available free of charge via the Internet at http://pubs.acs.org.

## ■ AUTHOR INFORMATION

### Corresponding Author

*E-mail: peteanu@andrew.cmu.edu.

### Present Addresses

[§]PPG Industries, 440 College Park Drive, Monroeville, PA,15146.

[‖]Center for Biomedical Engineering, Centennial Engineering Center, University of New Mexico, Albuquerque, NM 87131.

### Notes

The authors declare no competing financial interest.

## ■ ACKNOWLEDGMENTS

L.A.P. acknowledges NSF-CHE 079112 and CHE-1012529 for financial support. This work was partially performed at the Center for Integrated Nanotechnologies, a U.S. Department of Energy, Office of Basic Energy Sciences user facility at Los Alamos National Laboratory (contract DE-AC52-06NA25396), and Sandia National Laboratories (contract DE-AC04-94AL85000).

## ■ REFERENCES

(1) Gunes, S.; Heugebauer, H.; Sariciftci, N. S. *Chem. Rev.* **2007**, *107*, 1324.
(2) Thomas, S. W. I.; Joly, G. D.; Swager, T. M. *Chem. Rev.* **2007**, *107*, 1339.
(3) Schwartz, B. J. *Annu. Rev. Phys. Chem.* **2003**, *54*, 141.
(4) Schaller, R. D.; Lee, L. F.; Johnson, J. C.; Haber, L. H.; Saykally, R. J.; Vieceli, J.; Benjamin, I.; Nguyen, T.-Q.; Schwartz, B. J. *J. Phys. Chem. B* **2002**, *106*, 9496.
(5) Gao, Y.; Grey, J. K. *J. Am. Chem. Soc.* **2009**, *131*, 9654.
(6) Tenery, D.; Gesquiere, A. J. *Chem. Phys.* **2009**, *365*, 138.
(7) Hao, X.-T.; McKimmie, L.; Smith, T. A. *J. Phys. Chem. Lett.* **2011**, *2*, 1520.
(8) Peteanu, L. A.; Sherwood, G. A.; Werner, J. H.; Shreve, A. P.; Smith, T. M.; Wildeman, J. *J. Phys. Chem. C* **2011**, *115*, 15607.
(9) Vogelsang, J.; Brazard, J.; Adachi, T.; Bolinger, J. C.; Barbara, P. F. *Angew. Chem., Int. Ed.* **2011**, *50*, 2257.
(10) Traub, M. C.; Vogelsang, J.; Plunkett, K. N.; Nuckolls, C.; Barbara, P. F.; Vanden Bout, D. A. *ACS Nano* **2012**, *6*, 523.
(11) Yu, J.; Wu, C.; Tian, Z.; McNeill, J. *Nano Lett.* **2012**, *12*, 1300−1306.
(12) Oelkrug, D.; Egelhaaf, H.-J.; Gierschner, J.; Tompert, A. *Synth. Met.* **1996**, *76*, 249.
(13) Oelkrug, D.; Tompert, A.; Gierschner, J.; Engelhaaf, H.-J.; Hanack, M.; Hohloch, M.; Steinhuber, E. *J. Phys. Chem. B* **1998**, *102*, 1902.
(14) Collison, C. J.; Treemaneekarn, V.; Oldham, W. J., Jr.; Hsu, J. H.; Rothberg, L. J. *Synth. Met.* **2001**, *119*, 515.

(15) Landfester, K.; Montenegro, R.; Scherf, U.; Güntner, R.; Asawapirom, U.; Patil, S.; Neher, D.; Kietzke, T. *Adv. Mater.* **2002**, *14*, 651.
(16) Szymanski, C.; Wu, C.; Hooper, J.; Salazar, M. A.; Perdomo, A.; Dukes, A.; McNeill, J. *J. Phys. Chem. B* **2005**, *109*, 8543.
(17) Grey, J. K.; Kim, D. Y.; Norris, B. C.; Miller, W. L.; Barbara, P. F. *J. Phys. Chem. B* **2006**, *110*, 25568.
(18) Tretiak, S.; Saxena, A.; Martin, R. L.; Bishop, A. R. *J. Phys. Chem. B* **2000**, *104*, 7029.
(19) Cornil, J.; Beljonne, D.; Calbert, J.-P.; Bredas, J.-L. *Adv. Mater.* **2001**, *13*, 1053.
(20) Spano, F. C. *Annu. Rev. Phys. Chem.* **2006**, *57*, 217.
(21) Bittner, E. R.; Karabunarliev, S.; Herz, L. M. *J. Chem. Phys.* **2007**, *126*, 191102/1.
(22) Papadimitrakopoulos, F.; Yan, M.; Rothberg, L. J.; Katz, H. E.; Chandross, E. A.; Galvin, M. E. *Mol. Cryst. Liq. Cryst. Sci. Technol., Sect. A* **1994**, *256*, 663.
(23) Hu, D.; Yu, J.; Wong, K.; Bagchi, B.; Rossky, P. J.; Barbara, P. F. *Nature* **2000**, *405*, 1030.
(24) Wong, K. F.; Skaf, M. S.; Yang, C.-Y.; Rossky, P. J.; Bagchi, B.; Hu, D.; Yu, J.; Barbara, P. F. *J. Phys. Chem. B* **2001**, *105*, 6103.
(25) Sherwood, G. A.; Cheng, R.; Smith, T. M.; Werner, J. H.; Shreve, A. P.; Peteanu, L. A.; Wildeman, J. *J. Phys. Chem. C* **2009**, *113*, 18851.
(26) Sherwood, G. A.; Cheng, R.; Chacon-Madrid, K.; Smith, T. M.; Peteanu, L. A. *J. Phys. Chem. C* **2010**, *114*, 12078.